Viscosity and force corrections induced by the elimination of scales of motion in randomly forced turbulence

L. Machiels*
Fluid Mechanics Laboratory, Swiss Federal Institute of Technology, CH-1015 Lausanne, Switzerland
(Received 15 October 1997)

Systematic scale elimination in the description of randomly forced turbulence leads to a hierarchy of new terms in the dynamical equations. We consider two of these terms: the viscosity and random forcing corrections. We show how these corrections can be estimated using direct numerical simulation data of homogeneous isotropic turbulence. In the case of hyperviscous dissipation, the energy spectrum shows, between the inertial range and the dissipative range, an intermediate range characterized by a reduction of the eddy viscosity and a correction to the forcing representing a backward energy flux. [S1063-651X(98)02105-9]

PACS number(s): 47.27.Eq, 47.27.Gs

Several authors have proposed studying randomly forced turbulent flows [1–3]. Theoretical investigations (e.g., renormalization group) have focused on the incompressible Navier-Stokes equations forced by a Gaussian white-in-time noise term with a power-law correlation function in spectral space $\langle ff\rangle \propto k^{-y}$ [4–7]. These works explore the analogies between scalings in turbulence and scalings in field theory or critical phenomena [8]. In these theories, the scale-elimination procedure leads to an eddy viscosity, a force correction, a vertex correction and high-order terms (see Eyink [9]). Such types of randomly forced turbulent systems have been studied numerically by Machiels and Deville [10] for $y=3$. Note also that subgrid scale models including additive noise terms have been proposed recently (Carati *et al.* [11]). The aim of this paper is to present a simple mean-square algorithm suitable to compute, from the numerical data, the eddy viscosity and the correction to the forcing induced by scale elimination.

More precisely, we consider randomly forced turbulence described by the following equations:

$$\frac{\partial \boldsymbol{v}}{\partial t}+v_\beta\frac{\partial \boldsymbol{v}}{\partial x_\beta}=\boldsymbol{f}-\nabla p+(-1)^{h+1}\nu_h\nabla^{2h}\boldsymbol{v},\quad \nabla\cdot\boldsymbol{v}=0.$$

In these equations, $v_\alpha(\boldsymbol{x},t)$ $(\alpha=1,2,3)$ and $p(\boldsymbol{x},t)$ are respectively the velocity and pressure fields, $f_\alpha(\boldsymbol{x},t)$ is a solenoidal Gaussian white-noise forcing, h is a positive integer called the hyperviscosity index, and ν_h is the hyperviscosity parameter. The problem is defined on the domain $\mathcal{D}=]0,2\pi[^3$ with cyclic boundary conditions. We divide the field $\boldsymbol{v}$ into low-mode (or supergrid-mode) $\boldsymbol{v}^<$ and high-mode (or subgrid-mode) $\boldsymbol{v}^>$ components

$$\boldsymbol{v}^<(\boldsymbol{x},t)=\frac{1}{(2\pi)^3}\int_<\boldsymbol{v}(\boldsymbol{k},t)e^{i\boldsymbol{k}\cdot\boldsymbol{x}}d^3k,\quad \text{and}\quad \boldsymbol{v}^>=\boldsymbol{v}-\boldsymbol{v}^<,$$

where $\int_<$ means that the domain of integration is restricted to wave numbers $|\boldsymbol{k}|<k_c$ where k_c is a prescribed cutoff. The equations for the low modes may be written as

$$\frac{\partial \boldsymbol{v}^<}{\partial t}+\left(v_\beta^<\frac{\partial \boldsymbol{v}^<}{\partial x_\beta}\right)^<=\boldsymbol{f}^<-\nabla p^<+(-1)^{h+1}\nu_h\nabla^{2h}\boldsymbol{v}^<+\boldsymbol{g}^<,$$

$$\nabla\cdot\boldsymbol{v}^<=0,$$

where

$$\boldsymbol{g}=-v_\beta^<\frac{\partial \boldsymbol{v}^>}{\partial x_\beta}-v_\beta^>\frac{\partial \boldsymbol{v}^<}{\partial x_\beta}-v_\beta^>\frac{\partial \boldsymbol{v}^>}{\partial x_\beta}-\nabla p^>.$$

Note that $p^<$ is not defined by a spectral cutoff but is the pressure that ensures that $[v_\beta^<(\partial \boldsymbol{v}^</\partial x_\beta)]^<+\nabla p^<$ is solenoidal. We choose $p^>$ such that $\boldsymbol{g}$ is also solenoidal. The theory of scale elimination gives

$$\boldsymbol{g}^<(\boldsymbol{x},t)\overset{\text{law}}{=}\nabla^2\left[\int\int_0^\infty \nu_c(r,\tau)\boldsymbol{v}^<(\boldsymbol{x}-\boldsymbol{r},t-\tau)d\tau d^3r\right]+\boldsymbol{f}_c(\boldsymbol{x},t)+(\text{other interactions}),$$

where the symbol $\overset{\text{law}}{=}$ means the equality in a statistical sense (equality in probability). Some high-order interaction terms have been discussed by Rose [12] and Eyink [9]. In the present work, we focus on the eddy viscosity $\nu_c(r,\tau)$ and on the force correction $\boldsymbol{f}_c(\boldsymbol{x},t)$. The idea is to form the following functional:

$$\mathcal{F}[\nu_c(r,\tau),\boldsymbol{f}_c(\boldsymbol{x},t)]=\left\langle\left|\boldsymbol{g}^<(\boldsymbol{x},t)-\nabla^2\left[\int\int_0^\infty \nu_c(r,\tau)\times\boldsymbol{v}^<(\boldsymbol{x}-\boldsymbol{r},t-\tau)d\tau d^3r\right]-\boldsymbol{f}_c(\boldsymbol{x},t)\right|^2\right\rangle,$$

where $\boldsymbol{g}^<$, $\boldsymbol{v}^<$, and $\boldsymbol{f}_c$ are random and ν_c is deterministic. The symbol $\langle\ \rangle$ denotes the average. In this expression, $\boldsymbol{g}^<$ and $\boldsymbol{v}^<$ are obtained from numerical simulation results. Then, we seek to determine $\nu_c(r,\tau)$ and $\boldsymbol{f}_c(\boldsymbol{x},t)$, which minimize this functional, that is, such that

*Present address: Massachusetts Institute of Technology, Room 3-243, 77 Massachusetts Avenue, Cambridge, MA 02139.

TABLE I. Flow parameters.

	h	ν_h	E	ε	L	λ	τ_E	k_v	s_3	s_4
ST4	4	5.7×10^{-16}	0.42	0.158	0.969	0.084	1.82	110	−0.32	3.51
ST8	8	1.38×10^{-30}	0.42	0.16	0.956	0.092	1.807	85	−0.29	3.38
ST12	12	2.5×10^{-48}	0.432	0.159	0.968	0.072	1.803	107	−0.21	3.30

$$\frac{\delta\mathcal{F}[\nu_c(r,\tau),\boldsymbol{f}_c(\boldsymbol{x},t)]}{\delta\nu_c(r,\tau)}=0 \quad \text{and} \quad \frac{\delta\mathcal{F}[\nu_c(r,\tau),\boldsymbol{f}_c(\boldsymbol{x},t)]}{\delta\boldsymbol{f}_c(\boldsymbol{x},t)}=0.$$

This method is general in the sense that high-order interactions can also be taken into account and different minimization criteria (different functionals $\mathcal{F}$) can be implemented based on high-order statistics, for instance.

In practice, we work in Fourier space. The Fourier transform of the initial forcing is given by $\boldsymbol{f}(\boldsymbol{k},t)=\chi_0(k)\boldsymbol{h}(\boldsymbol{k},t)$ [e.g., $\chi_0^2(k)\propto k^{-y}$] where $k=|\boldsymbol{k}|$ and $\boldsymbol{h}(\boldsymbol{k},t)$ is an isotropic solenoidal Gaussian white-noise term defined by its correlation function

$$\langle h_\alpha(\boldsymbol{k}',t')h_\beta(\boldsymbol{k},t)\rangle=(2\pi)^3P_{\alpha\beta}(\boldsymbol{k})\,\delta(\boldsymbol{k}+\boldsymbol{k}')\,\delta(t-t'),$$

where $P_{\alpha\beta}(\boldsymbol{k})=\delta_{\alpha\beta}-k_\alpha k_\beta/k^2$. If we define $\widetilde{\boldsymbol{g}}(\boldsymbol{k},t)=\boldsymbol{g}(\boldsymbol{k},t)+\boldsymbol{f}(\boldsymbol{k},t)$, then we try to approximate $\widetilde{\boldsymbol{g}}^<(\boldsymbol{k},t)$ as

$$\widetilde{\boldsymbol{g}}^<(\boldsymbol{k},t)\approx\chi_c(k|k_c)\boldsymbol{h}^<(\boldsymbol{k},t)-\nu_c(k|k_c)k^2\boldsymbol{v}^<(\boldsymbol{k},t),$$

where the notation $k|k_c$ renders the dependence on the cutoff k_c explicit. As an additional assumption, we have removed the time dependence of ν_c, i.e., we have assumed $\nu_c(\boldsymbol{r},\tau)=\nu_c(\boldsymbol{r})\,\delta(\tau)$. This approximation, usually referred to as the Markovian approximation, assumes that the subgrid modes evolve more quickly than the supergrid modes. The functional $\mathcal{F}$ to be minimized reads

$$\mathcal{F}[\nu_c(k|k_c),\chi_c(k|k_c)]=\langle|\widetilde{\boldsymbol{g}}^<(\boldsymbol{k},t)+\nu_c(k|k_c)k^2\boldsymbol{v}^<(\boldsymbol{k},t)-\chi_c(k|k_c)\boldsymbol{h}^<(\boldsymbol{k},t)|^2\rangle.$$

In the implementation of the method, since we treat homogeneous isotropic turbulent problems and since the different realizations of the velocity field are taken in the statistically stationary regime, the symbol $\langle\ \rangle$ denotes the combination of a shell average and a time average. We compute

$$a(k)=2k^2\langle|\boldsymbol{v}^<(\boldsymbol{k},t)|^2\rangle,$$

$$b(k)=\langle\boldsymbol{v}^<(\boldsymbol{k},t)\cdot\boldsymbol{g}^{<*}(\boldsymbol{k},t)\rangle+\langle\boldsymbol{v}^{<*}(\boldsymbol{k},t)\cdot\boldsymbol{g}^<(\boldsymbol{k},t)\rangle,$$

where the asterisk denotes the complex conjugate. The solution of the system $\delta\mathcal{F}/\delta\nu_c(k)=0$ and $\delta\mathcal{F}/\delta\chi_c(k)=0$ is given by

$$\nu_c(k|k_c)=\frac{b(k)}{4\pi k^4\chi_0^2(k)-a(k)}, \tag{1}$$

$$\chi_c(k|k_c)=\frac{\chi_0(k)\{k^2b(k)-2a(k)+8\pi k^4\chi_0^2(k)\}}{8\pi k^4\chi_0^2(k)-2a(k)}. \tag{2}$$

When the external forcing vanishes, $\chi_0(k)=0$, Eq. (1) is equivalent to the formula proposed by Domaradzki *et al.* [13] based on the energy transfer.

Different numerical simulations have been performed with a homogeneous isotropic forcing $\langle ff\rangle\propto\chi_o(k)^2\propto k^{-3}$. The spatial discretization of the equations is based on the classical Fourier spectral method. The time integration is performed by a second-order Runge-Kutta scheme (the details of the numerical method are presented in [10]). For each of the calculations, the resolution is 256^3 modes. The main features of the simulations are reported in Table I, where E and ε are respectively the mean energy and the mean dissipation rate, L is the integral length scale, λ is the Taylor microscale, τ_E is the turnover time, $k_v=(\varepsilon/\nu_h^3)^{1/(6h-2)}$ is the Kolmogorov wave number, and s_3 and s_4 are respectively the skewness and flatness of the velocity derivative $\partial u_1/\partial x_1$.

The energy spectra $E(k)$ and the rescaled energy fluxes $\Pi(k)/\ln(k)$ for each of the simulations are represented in Figs. 1(a) and 1(b) [recall that, due to the particular form of the forcing $\langle ff\rangle\propto k^{-3}$, the energy flux $\Pi(k)$ is expected to scale like $\Pi(k)\propto\ln(k)$]. The energy spectra present three regions, namely, from low wave numbers to high wave num-

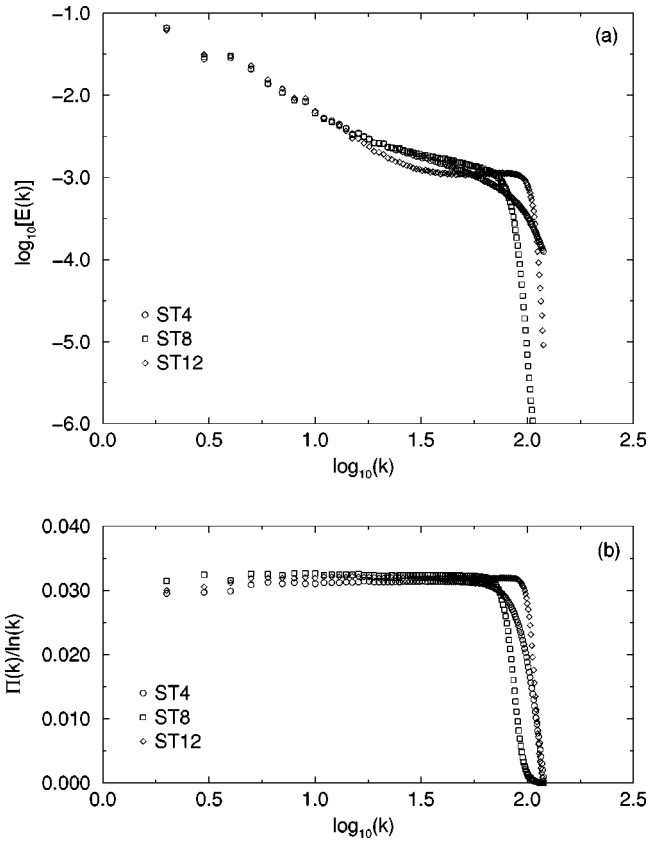

FIG. 1. Energy spectra (a) and rescaled energy fluxes (b) for the different simulations.

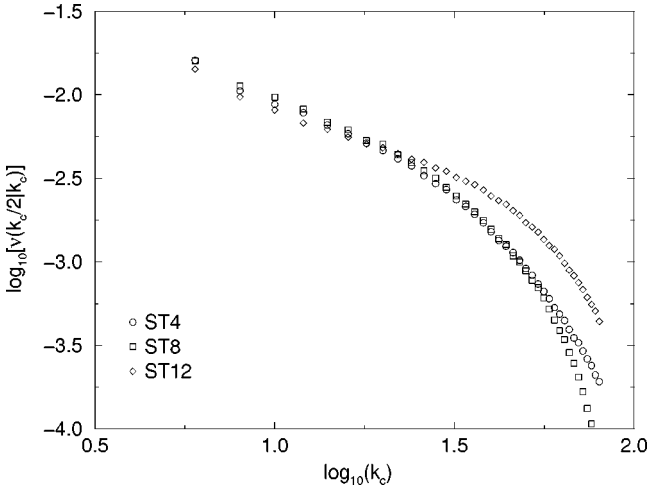

FIG. 2. Eddy viscosity $\nu_c(k_c/2|k_c)$ against the cutoff k_c for the different simulations.

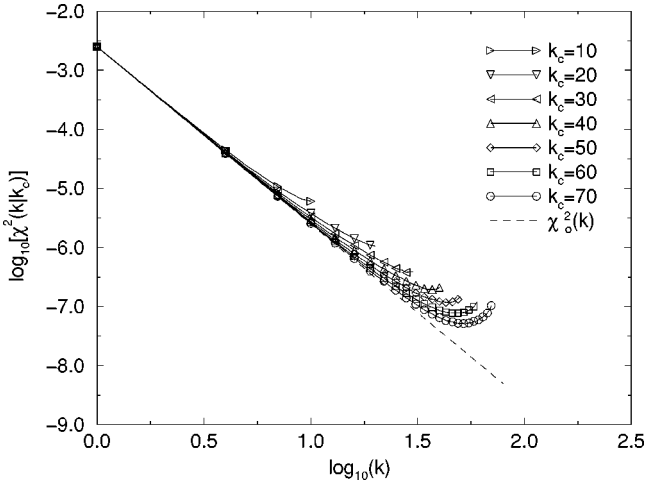

FIG. 4. Force correlation $\chi_c^2(k|k_c)$ for various cutoffs k_c (simulation ST4).

bers: (i) the inertial range, which is fairly independent of the dissipation mechanism; (ii) the intermediate range, characterized by a constant energy flux, but the energy spectrum is highly influenced by the type of dissipation mechanism; (iii) the dissipative range. The bump of energy in the intermediate range is usually referred to as the bottleneck deviation and has been previously observed and analyzed, for instance, in Falkovich [14], Sirovich *et al.* [15], and Lohse and Müller-Groeling [16].

We have applied Eqs. (1) and (2) to compute the viscosity $\nu_c(k|k_c)$ and force correlations $\chi_c^2(k|k_c)$ for $5 \leqslant k_c \leqslant 70$ and for the three simulations ST4, ST8, ST12. In Fig. 2, we present $\nu_c(k_c/2|k_c)$ as a function of k_c. We read the figure from right to left. We observe that, due to the different dissipation mechanisms, the eddy viscosity starts from different values at high wave numbers. The different curves for $\nu_c(k_c/2|k_c)$ go through a transient region, which corresponds roughly to the intermediate range. Then the three curves merge when they reach the inertial range, which confirms that this range is approximately independent of the dissipation mechanism.

Figure 3 shows the eddy viscosity $\nu_c(k|k_c)$ for simulation ST4. When the cutoff k_c is in or very close to the dissipative range (i.e., $50 \leqslant k_c \leqslant 70$), the eddy viscosity $\nu_c(k|k_c)$ rises sharply in the vicinity of the cutoff. This observation is consistent with the results of Domaradzki *et al.* [13]. The steep increase of eddy viscosity reduces as the cutoff is moved toward smaller wave numbers. For $20 \leqslant k_c \leqslant 40$, which corresponds roughly to the intermediate range, the eddy viscosity decreases slightly near the cutoff. For k_c below 10, it was difficult to have converged statistics since these shells contain only a few modes.

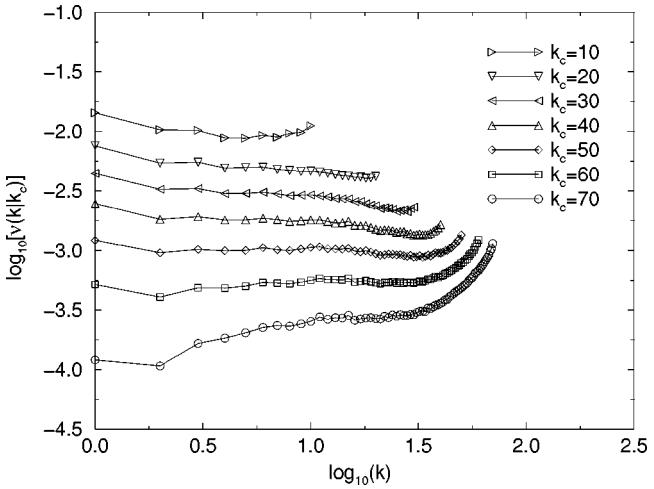

FIG. 3. Eddy viscosity $\nu_c(k|k_c)$ for various cutoffs k_c (simulation ST4).

The force correlations $\chi_c^2(k|k_c)$, represented in Fig. 4 for various cutoffs k_c, deviate from the initial forcing $\chi_0^2(k)$ near the cutoff. They present also a sharp rise, which reduces when the cutoff is moved towards small scales. In the intermediate range ($20 \leqslant k_c \leqslant 40$), the deviation is less pronounced but is present for a larger subrange of wave numbers than for $k_c > 50$. For a cutoff far in the dissipative range ($k_c \approx 80$), negative eddy viscosities have been observed for small k in conjunction with a considerable force correction, indicating an important reflection of the incidental flux of energy. Viscous simulations, not reported in this work, have shown the same behavior but for an extended cutoff range since the dissipative range is itself larger.

Simulation ST12 has a much more smaller dissipative range than simulation ST4 and, therefore, the intermediate range is clearly defined. In Fig. 5, the eddy viscosity $\nu_c(k|k_c)$ shows a more pronounced reduction near the cutoff than ST4 in the intermediate range ($k_c \geqslant 30$). For $k_c = 70$, a small bump appears near k_c that is due to the fact that we approach the dissipative range. For a cutoff at the border between the intermediate range and the inertial range ($k_c = 10$), the eddy viscosity increases near k_c, which is not unlike the cusp behavior predicted by some theories of isotropic turbulence. We remark that, for $k_c = 10$, the eddy viscosities are qualitatively the same for ST4 and ST12, this is not very apparent in the figures since the scalings are different. Note also that the $\nu_c(k|k_c)$ increases for small k. That is, most likely, an infrared cutoff effect.

The force correlations $\chi_c^2(k|k_c)$ in Fig. 6 do not present the sharp rise observed for ST4 which is associated to a cutoff in the dissipative range. As for the eddy viscosity, a

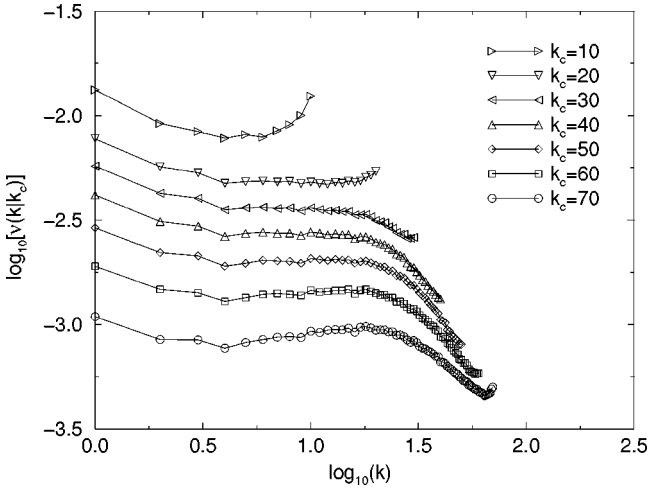

FIG. 5. Eddy viscosity $\nu_c(k|k_c)$ for various cutoffs k_c (simulation ST12).

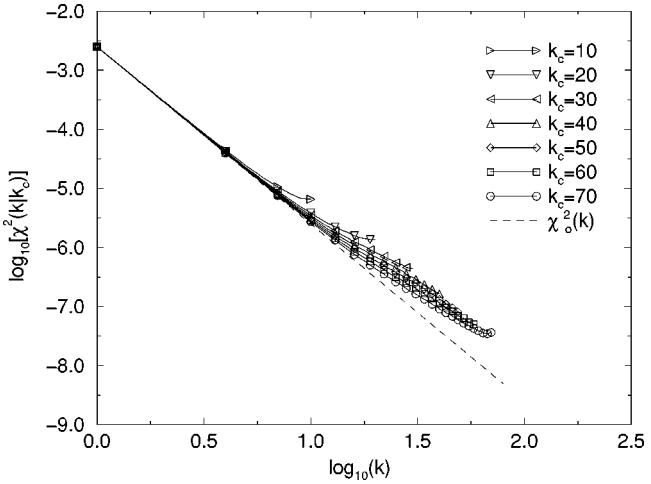

FIG. 6. Force correlation $\chi_c^2(k|k_c)$ for various cutoffs k_c (simulation ST12).

small bump appears for $k_c=70$. However, for k_c in the intermediate range, $\chi_c^2(k|k_c)$ shows a clear deviation from $\chi_0^2(k)$ for a significant range of wave numbers, which corresponds roughly to the intermediate range.

These observations are consistent with the following interpretation of the intermediate range bottleneck effect: the Kolmogorov spectrum is unstable near the dissipative range since it is too efficient in transferring energy to high wave numbers and leads to a system with a too low rate of energy dissipation. The effect is amplified as the hyperviscosity index is increased. The reaction of the system is to produce enough randomness in the intermediate range (as indicated by the values of the skewness s_3 and the flatness s_4 of the velocity derivative in Table I) to decrease the efficiency of transfer of energy in order to increase the level of energy and, therefore, the dissipation. Our observation that the eddy viscosity decreases agrees with the reduction of the efficiency of the energy transfer. It has been shown previously by Falkovich [14] that, in theory, the eddy viscosity decreases in the presence of molecular viscosity. The randomness arises from instabilities. The corrections to the random forcing may be attributed to a backward energy flux responsible for the destabilization of the flow structures in the intermediate range.

The simulations were performed on the computers of the Swiss Center for Scientific Computing, Manno. This research was supported by the Swiss National Foundation for Scientific Research.

[1] R. H. Kraichnan, J. Fluid Mech. **5**, 497 (1959).
[2] H. W. Wyld, Ann. Phys. (N.Y.) **14**, 143 (1961).
[3] E. A. Novikov, Zh. Eksp. Teor. Fiz. **47**, 1919 (1964) [Sov. Phys. JETP **20**, 1290 (1965)].
[4] D. Forster, D. R. Nelson, and M. J. Stephen, Phys. Rev. A **16**, 732 (1977).
[5] C. DeDominicis and P. C. Martin, Phys. Rev. A **19**, 419 (1979).
[6] V. Yakhot and S. A. Orszag, Phys. Rev. Lett. **57**, 1722 (1986).
[7] D. Ronis, Phys. Rev. A **36**, 3322 (1987).
[8] G. L. Eyink and N. Goldenfeld, Phys. Rev. E **50**, 4679 (1994).
[9] G. L. Eyink, Phys. Fluids **6**, 3063 (1994).
[10] L. Machiels and M. O. Deville (unpublished).
[11] D. Carati, S. Ghosal, and P. Moin, Phys. Fluids **7**, 606 (1995).
[12] H. A. Rose, J. Fluid Mech. **81**, 719 (1977).
[13] J. A. Domaradzki, R. W. Metcalfe, R. S. Rogallo, and J. J. Riley, Phys. Rev. Lett. **58**, 547 (1987).
[14] G. Falkovich, Phys. Fluids **6**, 1411 (1994).
[15] L. Sirovich, L. Smith, and V. Yakhot, Phys. Rev. Lett. **72**, 344 (1994).
[16] D. Lohse and A. Müller-Groeling, Phys. Rev. Lett. **74**, 1747 (1995).